

Coupling of symmetric and asymmetric modes in a high-power, high-efficiency traveling-wave amplifier

S. Banna and L. Schächter

Department of Electrical Engineering, Technion-Israel Institute of Technology, Haifa 32000, Israel

J. A. Nation and P. Wang

School of Electrical Engineering and Laboratory of Plasma Studies, Cornell University Ithaca, New York 14853

(Received 28 June 1999; revised manuscript received 1 December 1999)

A three-dimensional model has been developed for the investigation of the coupling of symmetric (TM_{01}) and asymmetric (HEM_{11}) modes in a high-power, high-efficiency traveling-wave amplifier. In the framework of a simplified model it is shown that the coupling between these two modes is determined by a single parameter that depends on the beam characteristics. For a specific set of parameters corresponding to operation at 35 GHz, simulations indicate that an initial HEM_{11} power of 0.5 MW at the input end is sufficient to deflect electrons to the wall. The build-up of this parasitic mode is investigated over many round trips of the wave in the structure and a threshold criterion for self-sustain oscillation is established. Finally a way for suppressing the HEM_{11} mode is analyzed.

PACS number(s): 41.75.Ht

INTRODUCTION

Theoretical analysis [1] and preliminary experimental studies [2] indicate that implementation of a 35 GHz traveling-wave amplifier based on a set of coupled cavities, is feasible. However, beam power requirements and technological constraints push the internal radius of the structure upwards such that when comparing the vacuum wavelength with a practical internal radius (R_{int}), we find that at the Ka band R_{int} is larger than the simple frequency scaling criterion dictates. For example, an X-band (say 11.66 GHz) structure may have a typical internal radius of 7 mm when driven by a beam of 3 mm radius. If we require comparable power levels carried by the beam for a system operating at the Ka band (35 GHz) then the beam radius can not be reduced below 2 mm and the internal radius of the structure may not be reduced below 3.5 mm. This radius is almost by 50% larger than the simple frequency scaling criterion implies.

The implications of large internal radius regarding operation with the symmetric TM_{01} mode, were discussed in Refs. [1] and [3]. In this study we shall focus our attention to the coupling with an *asymmetric* mode that may develop due to asymmetries of the electrons' distribution or asymmetries of the structure (e.g., feed system or output arm) or both. Such modes are called hybrid electric and magnetic (HEM) modes and the main problem associated with their presence, is their ability to deflect electrons to the wall. This phenomenon is well known in the accelerator community [4,5] under the name of beam break-up (BBU). On the other hand, big efforts are directed in the design of the next linear collider (NLC) acceleration structure in order to suppress these modes (see Ref. [6], and the references therein).

Recently, pulse shortening was observed in high-power traveling-wave amplifier experiments conducted at Cornell University [7] and this triggered the current study in which we examine to what extent the HEM_{11} mode contributes to the beam deflection to the wall in the course of beam-wave

interaction in a high-power, high-efficiency traveling-wave output structure. The build-up of asymmetric modes as a very narrow bunch traverses an acceleration structure is understood but, to the best of our knowledge, there is no equivalent analysis corresponding to a traveling-wave amplifier where the longitudinal bunch is of the order of the wavelength, its transverse size is several orders of magnitude larger in the amplifier case comparing to an accelerator and *collective* effects play a dominant role.

In this study we investigate the main aspects associated with the operation of a high-power traveling wave amplifier operating at 35 GHz taking into consideration also the lowest asymmetric mode (HEM_{11}). The extent the HEM_{11} mode is destructive, is quantified in terms of increase in the effective radius of the beam. We also examine the coupling of symmetric and asymmetric modes when the latter is selectively suppressed by specific suppression technique discussed at the end of this study.

3D QUASI-ANALYTIC MODEL

Suppose that a bunched beam, generated by either a series of cavities (klystron) or a slow wave structure, is injected into a uniform disk-loaded periodic structure. The structure is designed so that the phase velocity of the interacting wave generated by the bunched beam is synchronized to the average velocity of the electrons. The main interacting wave is the TM_{01} mode, but as mentioned before in the Introduction, due to asymmetry that may occur, we assume that one asymmetric mode may develop. According to the dispersion curves, the closest asymmetric mode to the TM_{01} that may interact with the beam is the low branch of the HEM_{11} mode. In order to analyze the system behaviors, we have to develop a set of equation describing the dynamics of the system. In this work we present a simple quasi-analytic model that enables quantitative analysis of the interaction of TM_{01} and the low branch of HEM_{11} in the presence of an electron beam in a traveling-wave amplifier. Within the framework of this

model the full three-dimensional (3D) motion of the particles is calculated and their effect on the electromagnetic field is assumed to be only in the longitudinal direction (1D). Additional assumptions of the model include: positive group velocity of both modes (TM₀₁ and HEM₁₁), their basic functional form is preserved, the energy conversion is primarily controlled by the longitudinal motion, and no electrons are reflected.

The total electromagnetic field propagating along the structure, is composed of three components, the rf field, the dc collective field (space charge), and the magnetic guiding field B_0 necessary for beam confinement. Bearing in mind that the system operates in steady state, assuming that it remains in a linear regime (single frequency) at all times, using the Poynting's theorem and the Newtonian equations of motion for the description of particle's dynamics, the governing equations read

$$\begin{aligned} \frac{d}{d\xi} \left(\frac{a_1}{\sqrt{\alpha_1}} \right) &= \sqrt{\alpha_1} \langle I_0(\bar{\Gamma}_1 \bar{r}_i) e^{-j\chi_{i,1}} \rangle_i, \\ \frac{d}{d\xi} \left(\frac{a_2}{\sqrt{\alpha_2}} \right) &= \sqrt{\alpha_2} \langle I_1(\bar{\Gamma}_2 \bar{r}_i) e^{-j\chi_{i,2} + j\phi_i} \rangle_i, \quad (1) \\ \frac{d}{d\xi} \chi_{i,1} &= \frac{\Omega_1}{\beta_{z,i}} - K_1, \quad \frac{d}{d\xi} \chi_{i,2} = \frac{\Omega_2}{\beta_{z,i}} - K_2, \\ \frac{d}{d\xi} \gamma_i &= -\frac{1}{2} [a_1 I_0(\bar{\Gamma}_1 \bar{r}_i) e^{j\chi_{i,1}} + a_2 I_1(\bar{\Gamma}_2 \bar{r}_i) e^{j\chi_{i,2} - j\phi_i} + \text{c.c.}], \\ \frac{d}{d\xi} \bar{x}_i &= \frac{\beta_{x,i}}{\beta_{z,i}}, \quad \frac{d}{d\xi} \bar{y}_i = \frac{\beta_{y,i}}{\beta_{z,i}}, \\ \frac{d}{d\xi} \bar{p}_{x,i} &= -\Omega_c \frac{\bar{p}_{y,i}}{\bar{p}_{z,i}} + \Omega_p^2 \frac{\bar{x}_i}{\gamma_{z,i}^2 \beta_{z,i}} + \frac{\bar{F}_x^{(rf)}}{\beta_{z,i}}, \\ \frac{d}{d\xi} \bar{p}_{y,i} &= \Omega_c \frac{\bar{p}_{x,i}}{\bar{p}_{z,i}} + \Omega_p^2 \frac{\bar{y}_i}{\gamma_{z,i}^2 \beta_{z,i}} + \frac{\bar{F}_y^{(rf)}}{\beta_{z,i}}, \\ \bar{p}_{z,i} &= \sqrt{\gamma_i^2 - \bar{p}_{x,i}^2 - \bar{p}_{y,i}^2}. \end{aligned}$$

In this set of equations the first two lines include the amplitude dynamics equations, followed by the phase dynamics equations and the single-particle energy conservation, the last four lines represent the dynamics equations of the particles' transversal location and their normalized momentum $\bar{p}_{x,i} \equiv \gamma_i \beta_{x,i}$, $\bar{p}_{y,i} \equiv \gamma_i \beta_{y,i}$, and $\bar{p}_{z,i} \equiv \gamma_i \beta_{z,i}$; indices 1 and 2 represent the TM₀₁ and HEM₁₁ modes correspondingly; $\langle \dots \rangle$ represents averaging over entire ensemble of particles. The other definitions used here are $\xi \equiv z/d$, $\bar{x} \equiv x/d$, $\bar{y} \equiv y/d$, d is the total interaction length, $\Omega \equiv \omega d/c$, $\Omega_c \equiv ecB_0 d/mc^2$,

$$\Omega_p^2 \equiv \frac{I \eta_0}{mc^2/e} \frac{d^2}{\pi R_{\text{beam}} \beta_{ph}},$$

$K \equiv kd$, $a \equiv eEd/mc^2$, $\gamma_i = (1 - \bar{\beta}^2)^{-1/2}$, $\chi_{i,1}$ is the phase of the i th particle relative to the TM₀₁ mode whereas $\chi_{i,2}$ is the phase of the same particle relative to the HEM₁₁ mode; ϕ_i is

the azimuthal location of the i th particle; α_1, α_2 are the coupling coefficients defined as $\alpha_\mu \equiv (eIZ_{\text{int}}^\mu/mc^2)(d^2/\pi R_{\text{int}}^2)$, $\mu = 1, 2$; $\bar{\Gamma} \equiv \sqrt{K^2 - \Omega^2}$ and $\bar{r} \equiv r/d$. R_{beam} is the radius of the beam at the input where it was injected. The interaction impedance is defined as $Z_{\text{int}} \equiv (\pi R_{\text{int}}^2) |\mathcal{E}|^2 / 2P$, where \mathcal{E} is the amplitude of the zero's harmonic of the appropriate mode and P is the total power that flows in the system in the specific mode. In principle, the coupling coefficient α and the wave number K may vary in space, however, in the results that follow, we shall assume that the structure is uniform. The normalized rf forces calculated using Lorentz force law are defined as follows:

$$\begin{aligned} \bar{F}_{x,i}^{(rf)} &\equiv \frac{F_x^{(rf)} d}{mc^2} = A \left\{ [I_0(\bar{\Gamma}_1 \bar{r}_i) \text{Re}(ja_1 e^{j\chi_{i,1}}) \right. \\ &\quad + I_1(\bar{\Gamma}_2 \bar{r}_i) \text{Re}(ja_2 e^{j\chi_{i,2} - j\phi_i})] \cos(\phi_i) \\ &\quad \left. - \frac{I_1(\bar{\Gamma}_2 \bar{r}_i)}{\bar{\Gamma}_2 \bar{r}_i} \text{Re}(a_2 e^{j\chi_{i,2} - j\phi_i}) \sin(\phi_i) \right\} \\ &\quad + B \left\{ \left[\frac{I_2(\bar{\Gamma}_2 \bar{r}_i)}{\bar{\Gamma}_2 \bar{r}_i} \text{Re}(ja_2 e^{j\chi_{i,2} - j\phi_i}) \right] \cos(\phi_i) \right. \\ &\quad \left. - I_1(\bar{\Gamma}_2 \bar{r}_i) \text{Re}(a_2 e^{j\chi_{i,2} - j\phi_i}) \sin(\phi_i) \right\} \\ \bar{F}_{y,i}^{(rf)} &\equiv \frac{F_y^{(rf)} d}{mc^2} = A \left\{ [I_0(\bar{\Gamma}_1 \bar{r}_i) \text{Re}(ja_1 e^{j\chi_{i,1}}) \right. \\ &\quad + I_1(\bar{\Gamma}_2 \bar{r}_i) \text{Re}(ja_2 e^{j\chi_{i,2} - j\phi_i})] \sin(\phi_i) \\ &\quad \left. + \frac{I_1(\bar{\Gamma}_2 \bar{r}_i)}{\bar{\Gamma}_2 \bar{r}_i} \text{Re}(a_2 e^{j\chi_{i,2} - j\phi_i}) \cos(\phi_i) \right\} \\ &\quad + B \left\{ \left[\frac{I_1(\bar{\Gamma}_2 \bar{r}_i)}{\bar{\Gamma}_2 \bar{r}_i} \text{Re}(ja_2 e^{j\chi_{i,2} - j\phi_i}) \right] \sin(\phi_i) \right. \\ &\quad \left. + I_1(\bar{\Gamma}_2 \bar{r}_i) \text{Re}(a_2 e^{j\chi_{i,2} - j\phi_i}) \cos(\phi_i) \right\}, \quad (2) \end{aligned}$$

where $A \equiv -\gamma_{ph}(1 - \beta_{z,i}\beta_{ph})$; $B \equiv -j\mathcal{H}_0\gamma_{ph}(\beta_{ph} - \beta_{z,i})$, and $\mathcal{H}_0 \equiv \eta_0 \mathcal{H}_2 / \mathcal{E}_2$ where \mathcal{H}_2 is the magnetic field amplitude of zero's harmonic of the HEM₁₁ mode; β_{ph} is the phase velocity of both modes.

SIMULATION RESULTS AND DISCUSSION

Let us first consider the coupling between the modes due to an asymmetry in the beam, ignoring the transverse motion. This enables to determine the spatial growth of the combined modes. Based on Eq. (1), the *spatial growth* of the system may be deduced by taking twice the derivative of the amplitude equation and substituting in the equation of the motion; the result is

$$\begin{aligned} \frac{d^3 a_1}{d\xi^3} + \frac{j}{2} [(\alpha_1 \Omega_1 p_1) a_1 + (\alpha_1 \Omega_1 U) a_2] \\ \cong -\alpha_1 \left\langle \left(\frac{\Omega_1}{\beta_i} - K_1 \right)^2 e^{-j\chi_{i,1}} I_0(\bar{\Gamma}_1 \bar{r}_i) \right\rangle, \\ \frac{d^3 a_2}{d\xi^3} + \frac{j}{2} [(\alpha_2 \Omega_2 p_2) a_2 + (\alpha_2 \Omega_2 U^*) a_1] \\ \cong -\alpha_2 \left\langle \left(\frac{\Omega_2}{\beta_i} - K_2 \right)^2 e^{-j\chi_{i,2} + j\phi_i} I_1(\bar{\Gamma}_2 \bar{r}_i) \right\rangle, \end{aligned} \quad (3)$$

where

$$\begin{aligned} p_1 &\equiv \langle I_0^2(\bar{\Gamma}_1 \bar{r}_i) (\gamma_i \beta_i)^{-3} \rangle, \\ U &\equiv \langle e^{-j(\chi_{i,1} - \chi_{i,2} + \phi_i)} (\gamma_i \beta_i)^{-3} I_0(\bar{\Gamma}_1 \bar{r}_i) I_1(\bar{\Gamma}_2 \bar{r}_i) \rangle, \\ p_2 &\equiv \langle I_1^2(\bar{\Gamma}_2 \bar{r}_i) (\gamma_i \beta_i)^{-3} \rangle \end{aligned}$$

and the terms where the phase varies rapidly were neglected. Ignoring the two ‘‘noise’’ terms in the right hand side of both equations, we may calculate the eigenwave number of the coupled system, by assuming solutions of the form $a_1 = \bar{a}_1 e^{-jS\xi}$ and $a_2 = \bar{a}_2 e^{-jS\xi}$, hence

$$\begin{pmatrix} S^3 + \frac{1}{2} \alpha_1 \Omega_1 p_1 & \frac{1}{2} \alpha_1 \Omega_1 U \\ \frac{1}{2} \alpha_2 \Omega_2 U^* & S^3 + \frac{1}{2} \alpha_2 \Omega_2 p_2 \end{pmatrix} \begin{pmatrix} \bar{a}_1 \\ \bar{a}_2 \end{pmatrix} = 0. \quad (4)$$

As clearly revealed by this matrix, the term U represents the coupling between the cold-structure eigenmodes (TM_{01} and HEM_{11}). From its definition it is realized that U is determined by the correlation between the two phases ($\chi_{i,1}, \chi_{i,2}$) and also by the correlation of the azimuthal, radial and momentum distribution of the electrons. When the coupling between the modes is zero, each one of the modes (TM_{01} and HEM_{11}) develops independently according to $S^3 + S_1^3 = 0$ or $S^3 + S_2^3 = 0$ where $S_\mu^3 \equiv \frac{1}{2} \alpha_\mu \Omega_\mu p_\mu$. As evident from Eq. (3) the coupling between the TM_{01} and HEM_{11} is controlled by a single parameter

$$\begin{aligned} \bar{u} &= \sqrt{\frac{UU^*}{p_1 p_2}} \\ &= \frac{|\langle e^{-j(\chi_{i,1} - \chi_{i,2} + \phi_i)} (\gamma_i \beta_i)^{-3} I_0(\bar{\Gamma}_1 \bar{r}_i) I_1(\bar{\Gamma}_2 \bar{r}_i) \rangle|}{\sqrt{\langle I_0^2(\bar{\Gamma}_1 \bar{r}_i) (\gamma_i \beta_i)^{-3} \rangle \langle I_1^2(\bar{\Gamma}_2 \bar{r}_i) (\gamma_i \beta_i)^{-3} \rangle}} \end{aligned} \quad (5)$$

since the solution of the coupled system can be determined from $S^3 + S_\pm^3 = 0$, where

$$S_\pm^3 = -\frac{1}{2} (S_1^3 + S_2^3) \pm \frac{1}{2} \sqrt{(S_1^3 - S_2^3)^2 + 4S_1^3 S_2^3 \bar{u}^2}. \quad (6)$$

In these expressions S_+ corresponds to the HEM_{11} -like solution since at the limit $\bar{u} = 0, S_+ = S_2$ whereas S_- corresponds to the TM_{01} -like solution.

The solid-lines in Fig. 1 illustrate the variation of the

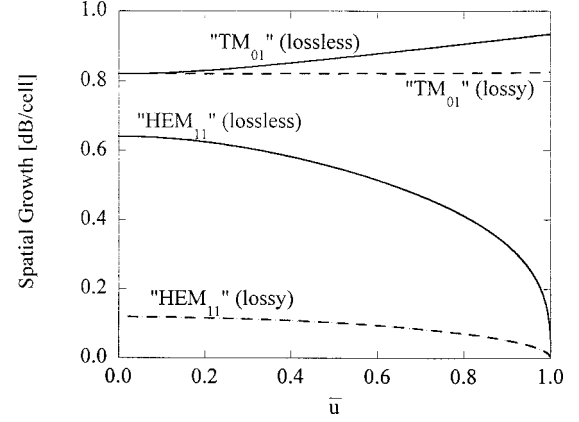


FIG. 1. The spatial growth per cell versus the coupling parameter \bar{u} as defined in Eq. (5). Solid line: growth rate without HEM mode damping. Dashed line: spatial growth with HEM mode damping ($\sigma \approx 0.05$).

growth per cell $g_\pm \equiv (L/d) 20 \log_{10}(e^{\sqrt{3}S_\pm/2})$ as a function of the parameter \bar{u} . The parameters in this simulation are $I = 300$ A, $V = 850$ kV, $R_{\text{int}} = 3.5$ mm, $R_{\text{ext}} = 5$ mm, $R_b = 2$ mm, $L = 1.98$ mm, $f_{\text{TM}_{01}} = 35$ GHz, $f_{\text{HEM}_{11}} = 38.63$ GHz, $Z_{\text{int}}^{\text{TM}_{01}} = 374 \Omega$, $Z_{\text{int}}^{\text{HEM}_{11}} = 1.61$ k Ω , and it was assumed that the electrons have a vanishingly small velocity spread. When the modes are completely correlated ($\bar{u} = 1$) the spatial growth of the HEM_{11} -like mode is zero whereas the TM_{01} -like is slightly larger than the case when there is no coupling ($\bar{u} = 0$). Although, the HEM_{11} -like wave becomes unimportant, we have to remember that the TM_{01} -like mode is not a pure TM_{01} mode but rather a hybrid of TM_{01} and HEM_{11} therefore, the impact of the HEM's components are destructive since it has the same spatial growth as the pure TM_{01} —they share the same eigen wave number. In order to illustrate the impact of these two coupled modes on the beam, we consider next the 3D model that enables to examine the development of the beam expansion.

Figure 2 shows the build-up of the HEM_{11} power at the input versus the number of round trips for several values of the overall reflection coefficient ρ (output and input end) of

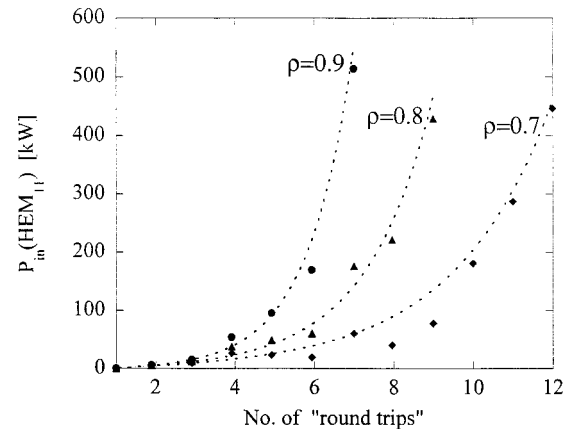


FIG. 2. The HEM_{11} input power for several overall reflection coefficients (ρ), versus number of round trips during the pulse duration. During one pass the efficiency of energy conversion into the TM mode approaches the 70% level.

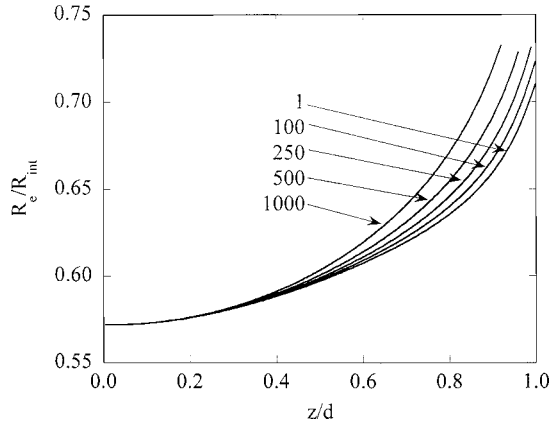


FIG. 3. The radius of the envelope for several HEM₁₁ power levels at the input (kW).

the structure. The TM₀₁ mode is generated by a modulated $|\chi_{i,1}| < 7\pi/18$ beam and it reaches efficiencies of 70%; the other parameters are as above and in addition $d = 2.3$ cm. Clearly for sufficiently high overall reflection coefficient ρ , the power at the input reaches the 0.5 MW level after order of 10 round trips in the structure. Here it is tacitly assumed that it is difficult to tune the structure at both frequencies (of TM and HEM). Consequently, since the structure is tuned to the frequency of the TM₀₁ mode, the reflection coefficient of the HEM mode from both ends of the structure is expected to be relatively large; values of 0.7–0.9 are feasible.

Based on these arguments we may evaluate the threshold current necessary for the occurrence of self-sustain oscillation of the HEM mode. If the amplitude of the latter at the input end is A_2 , then at the output end it reads $A_2 e^{-jK_2(e^{-jS_+}/3)}$ —see Ref. [8]; at this point the wave is reflected (ρ_{out}) towards the input end. As it reaches the starting point, the amplitude of the wave reads $A_2 e^{-jK_2(e^{-jS_+}/3)} \rho_{\text{out}} e^{-jK_2} \rho_{\text{in}}$. Ignoring ohmic loss, self-sustain oscillation may occur if the absolute value of this quantity is larger than $|A_2|$ consequently, the threshold value is determined by the condition $\text{Im}(S_+) = -\ln(\rho/3)$ where the overall reflection coefficient associated with the HEM mode is $\rho \equiv |\rho_{\text{in}} \rho_{\text{out}}|$. An upper limit of the threshold current may be evaluated if we note (based on Fig. 1) that $\text{Im}(S_+) \approx \text{Im}(S_1)$, namely, the spatial growth rate of the combined modes is similar to that of the TM₀₁ in the absence of coupling. As a result, the necessary condition for avoiding self-sustained oscillation reads

$$I \leq I_{\text{th}} \approx \left[\frac{-2}{\sqrt{3}} \ln\left(\frac{\rho}{3}\right) \right]^3 \frac{2}{\Omega_1 p_1} \frac{\pi P_{\text{int}}^2}{d^2} \frac{mc^2/e}{Z_{\text{int}}^{\text{TM}_{01}}}. \quad (7)$$

The overall reflection coefficient (ρ) is directly related to the quality factor $[Q^{\text{HEM}}]$ of the structure by $\rho = \sqrt{(Q^{\text{HEM}} \beta_{\text{gr}}^{\text{HEM}} / \Omega_2 - 1) / (Q^{\text{HEM}} \beta_{\text{gr}}^{\text{HEM}} / \Omega_2 + 1)}$ where $\beta_{\text{gr}}^{\text{HEM}}$ is the normalized group velocity of the HEM mode. In order to have a measure as of this threshold current we calculated the values corresponding to the simulation results presented in Fig. 2. Their values are $I_{\text{th}}(\rho = 0.9) = 360$ A, $I_{\text{th}}(\rho = 0.8) = 480$ A, and $I_{\text{th}}(\rho = 0.7) = 640$ A; in case of a modulated beam these values may be readily exceeded.

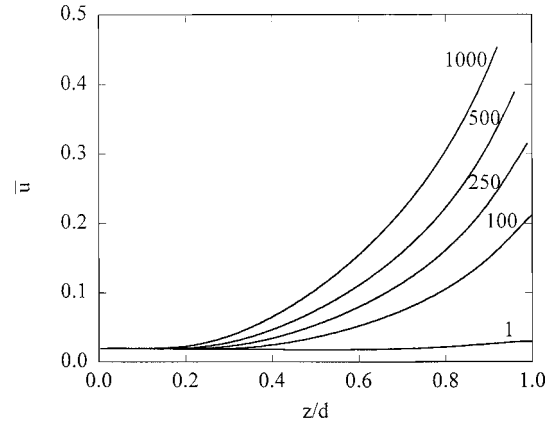


FIG. 4. The coupling parameter for several HEM₁₁ power levels at the input (kW).

Accumulation of electromagnetic power in the asymmetric mode causes beam's expansion and eventually electrons may hit the structure's wall. In order to examine this process we shall consider next the interaction during a single pass for a specific HEM power at the input end, allowing transverse motion. Figure 3 shows the radius of beam's envelope $R_e/R_{\text{int}} \equiv 2(d/R_{\text{int}}) \langle \bar{r}_i \rangle$, for several initial HEM₁₁ power levels at the input; the simulation is terminated if one particle hits the internal radius of the structure. In order to observe the correlation between this quantity and the coupling parameter $\bar{\mu}$, defined in the context of the 3D model, we plot in Fig. 4 the latter for the same simulation. As revealed by these two figures, the correlation between beam's envelope and the coupling parameter is evident. Moreover, since for $P_{\text{in}}^{\text{HEM}} = 0.5$ MW the simulation terminates before the end of the structure ($z = d$), clearly there are particles that hit the structure. It is important to emphasize that the beam expands even

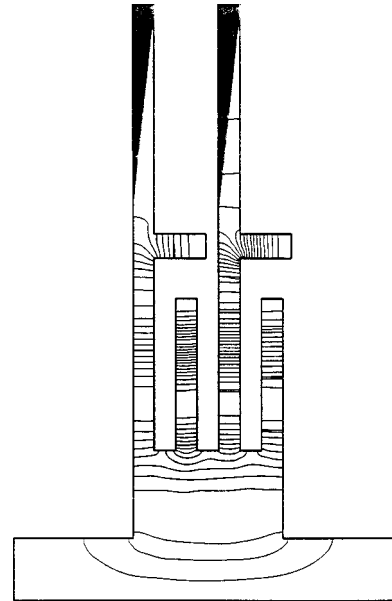


FIG. 5. SUPERFISH simulation of a set of choked loaded cavities used to form a periodic structure (periodicity of 1.8 mm, disk thickness of 0.9 mm, phase advance per cell of $\pi/2$, internal radius of 6 nm and stub of 2.2 nm). The system is designed to operate at 35 GHz.

when the HEM_{11} is “turned off,” however, with the latter “on,” its expansion speeds up.

It is evident from the former results that the HEM_{11} mode plays a destructive role during the interaction process. For suppression of the HEM_{11} mode, *selective* damping may be introduced, i.e., that is a damping mechanism that is transparent to TM_{01} mode [3,9]. This can be represented by a damping parameter, σ , that in the absence of the beam, causes a decay corresponding to $e^{-\xi/\sigma}$. Consequently, in the amplitude equation of the HEM_{11} mode we may replace $d\bar{a}_2/d\xi \rightarrow d\bar{a}_2/d\xi + (1/\sigma)\bar{a}_2$. Following the same approach as before we find instead of Eq. (4)

$$\begin{pmatrix} S^3 + \frac{1}{2}\alpha_1\Omega_1 p_1 & \frac{1}{2}\alpha_1\Omega_1 U \\ \frac{1}{2}\alpha_2\Omega_2 U^* & S^3 + \frac{j}{\sigma}S^2 + \frac{1}{2}\alpha_2\Omega_2 p_2 \end{pmatrix} \begin{pmatrix} \bar{a}_1 \\ \bar{a}_2 \end{pmatrix} = 0. \quad (8)$$

The dashed lines in Fig. 1 illustrate the spatial growth per cell (in dB) in the case of damping the HEM mode ($\sigma \approx 0.05$ corresponding to 15 dB per cell in the absence of the beam). Two facts are evident: first, the HEM_{11} -like mode is substantially suppressed though as well known in traveling wave tubes role that the damping of the active interaction is lower than the cold attenuation. Secondly, the TM_{01} -like mode is almost independent of the \bar{u} indicating that the TM_{01} -like is close to the pure TM_{01} mode.

This type of damping may be accomplished by a series of choked loaded [10] cavities. These have high quality factor (Q) at the frequency that corresponds to the TM_{01} mode and low Q otherwise. Alternative ways of suppression of HEM modes were discussed in Refs. [6, 11, 12] and they include incoherence of the structure, namely, a structure that looks periodic to the symmetric mode but nonperiodic to the asymmetric one.

In order to illustrate the potential of a series of a choked loaded cavities for the mode suppression we examined an “open cavity” with stub tuner. For this example we consider only symmetric modes thus we use SUPERFISH to calculate the first four resonances and corresponding quality factors; the electric field distribution at 34.8 GHz is illustrated in Fig. 5. The quality factor at 34.826 GHz was found to be 1720 whereas at three other eigenfrequencies 11.1, 22.8, and 44.4 GHz, the quality factor is at least one order of magnitude smaller, namely, 60, 72, and 112 correspondingly. Although these are only symmetric TM modes, we anticipate a similar behavior for nonsymmetric modes.

CONCLUSIONS

In conclusion, the design of a high-power, high-efficiency traveling-wave output structure should account for the effect of the asymmetric modes that the beam may interact with. The coupling between the symmetric and asymmetric modes was shown to be controlled, in the 3D case, by a single parameter [see Eq. (5)] that reveals good correlation with HEM_{11} buildup. When substantial power associated with the HEM_{11} mode accumulates in the output structure, it may cause deflection of the beam to the wall. A threshold criterion was established for the condition (current) necessary for self-sustain oscillation of the HEM_{11} mode to occur. And finally a way for suppressing the HEM_{11} mode using choke mode cavity was introduced.

ACKNOWLEDGMENT

This study was supported by the U.S. Department of Energy and the Binational Science Foundation of United States and Israel.

[1] L. Schächter and J. A. Nation, *Phys. Rev. E* **57**, 7176 (1998).
 [2] Cz. Golkowski, J. D. Ivers, J. A. Nation, P. Wang, and L. Schächter (unpublished).
 [3] S. Banna, J. A. Nation, L. Schächter, and P. Wang (unpublished).
 [4] W. K. H. Panofsky and W. A. Wenzel, *Rev. Sci. Instrum.* **27**, 967 (1956).
 [5] R. H. Helm and G. Loew, in *Linear Accelerators*, edited by P. M. Lapostolle and A. L. Septier (North-Holland, Amsterdam, 1970), p. 173.

[6] R. M. Jones, N. M. Kroll, and R. H. Miller (unpublished).
 [7] P. Wang, J. D. Ivers, J. A. Nation, S. Banna, and L. Schächter (unpublished).
 [8] *Beam-Wave Interaction in Periodic and Quasi-Periodic Structures* (Springer-Verlag, Heidelberg, 1997), p. 156.
 [9] L. Schächter, S. Banna, and J. A. Nation (unpublished).
 [10] T. Shintake, *Jpn. J. Appl. Phys.* **31**, 1567 (1992).
 [11] J. Haimson and B. Meklenburg (unpublished).
 [12] J. Haimson and B. Meklenburg (unpublished).